

3. J. E. Keffer and W. D. Baines, *J. Fluid Mech.*, **15**, No. 4, 481-496 (1963).
4. S. T. Kashafutdinov, *Izv. Sib. Otd. AN SSSR, Ser. Tekh. Nauk*, **2**, No. 8, 26-32 (1971).
5. I. B. Palatnik and D. Zh. Temirbaev, in: *Problems of Heat and Power Engineering and Applied Thermophysics [in Russian]*, No. 4, Alma-Ata (1967), pp. 99-105.
6. L. N. Voitovich, T. A. Girshovich, and N. P. Korzhov, *Izv. Akad. Nauk SSSR, Mekh. Zhidk. Gaza*, No. 5, 151-155 (1978).
7. L. N. Voitovich, T. A. Girshovich, and N. P. Korzhov, in: *Turbulent Jet Flows [in Russian]*, Tallinn (1979), pp. 158-165.
8. G. N. Abramovich, T. A. Girshovich, S. Yu. Krashenninikov, et al., *Theory of Turbulent Jets [in Russian]*, Moscow (1984).
9. Patankar, Basu, and Alpey, *Trans. ASME, Ser. D, J. Basic Eng.*, No. 4 (1977).
10. A. L. Dorfman, *Izv. Akad. Nauk SSSR, Mekh. Zhidk. Gaza*, No. 2, 181-185 (1978).
11. G. N. Abramovich, *Theory of Turbulent Jets [in Russian]*, Moscow (1960).

EFFECT OF BODY SHAPE ON THE CHARACTERISTICS
OF A SELF-SIMILAR PLANE WAKE

P. Ya. Cherepanov and Yu. M. Dmitrenko

UDC 532.517.4

The turbulence characteristics in the wake of an elongated plane body with two sharp trailing edges have been experimentally investigated. It is shown that in the self-similar region the parameters of the plane wake depend on the body shape.

It is known [1] that for fairly large Reynolds numbers $Re = U_\infty d/\nu$ and at large distances x_1/d from the body various types of turbulent wakes develop self-similarly. This means that the statistical turbulence characteristics, which are determined by the large-scale components of the motion, can be represented in the form:

$$\Delta U = U_* f(x_2/l_*); \overline{u_i u_j} = U_*^2 g_{ij}(x_2/l_*) \text{ etc.} \quad (1)$$

Here, $\Delta U = U - U_\infty$ is the average longitudinal velocity defect in the wake; $\overline{u_i u_j}$ are the components of the Reynolds stress tensor. In (1) the characteristic scales of velocity U_* and length l_* depend only on the longitudinal coordinate x_1 , the free-stream velocity U_∞ and the drag $F = C_x \rho U_\infty^2 S/2$.

In the case of a plane wake U_* and l_* are given by

$$U_* = U_\infty \left[\frac{C_x d}{2(x_1 + x_0)} \right]^{0.5}; l_* = [0.5 C_x d (x_1 + x_0)]^{0.5}, \quad (2)$$

where x_0 is the virtual origin.

For a long time it was considered [1, 2] that in the region in which the flow in the wake is self-similar the statistical turbulence characteristics can be completely determined by specifying the drag, the free-stream flow velocity U_∞ and the position of the virtual origin x_0 . In other words, the functions f , g_{ij} , etc. in Eqs. (1) were assumed to be universal, i.e., not to depend on the body shape. Then, in a series of experimental studies [3-5] it was shown that the structure of the axisymmetric wake depends not only on the drag and the free-stream velocity but also on the shape of the body. As far as the plane wake is concerned, the hypothesis of the universality of the characteristics in the self-similar flow region is so far considered to be correct [2]. Despite the fact that the hypothesis was partially confirmed in [6] by comparing the results of measurements in the wakes of circular and elliptical cylinders, there is reason to doubt its applicability to all plane bodies without exception. In particular, in [7] it was shown that in the wake of an elongated plane body with two sharp trailing edges the shape of the self-similar average longitudinal velocity profile differs significantly from the so-called universal profile observed in the wake

A. V. Lykov Institute of Heat and Mass Transfer, Academy of Sciences of the Belorussian SSR, Minsk. Translated from *Inzhenerno-Fizicheskii Zhurnal*, Vol. 54, No. 6, pp. 912-919, June, 1988. Original article submitted December 30, 1986.

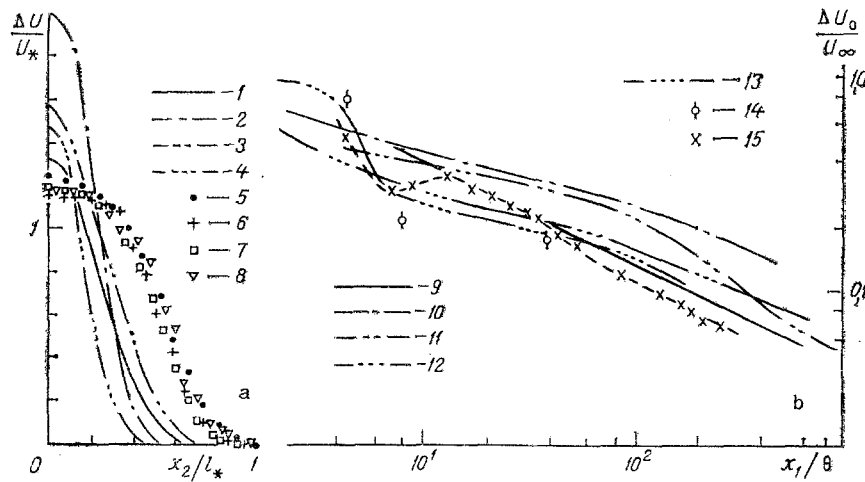


Fig. 1. Self-similarity profiles (a) and variation along the wake axis (b) of the average longitudinal velocity defect: 1) circular cylinder [1]; 2) plate [13]; 3) circular cylinder [11]; 4) elliptic cylinder [6]; 5-8) authors' data ($x_1/d = 38, 48, 58, \text{ and } 60$ respectively); 9) circular cylinder [10]; 10) plate [13]; 11) plate [15]; 12) plate [14]; 13) cylinder [14]; 14) cylinder [12]; 15) authors' data.

of a plate, a circular cylinder, etc. The present study is a continuation of [7]. Its object is to obtain detailed experimental information on the mean and fluctuation characteristics in the turbulent wake of an elongated plane body with two sharp edges and to compare it with the analogous characteristics of various plane wakes.

The experiments were carried out in a wind tunnel with a closed working section measuring $80 \times 80 \times 1200$ mm. A plane body in the form of a rectangular hollow wing with a symmetric profile was mounted horizontally at zero angle of attack at the beginning of the working section. The span was equal to 0.074 m, the chord to 0.1 m, and the maximum thickness $d = 0.01$ m. Along the trailing edge of the model there was a slit 0.002 m wide, through which it was possible to blow a jet and thereby modify the excess momentum. The results of investigating a plane wake with zero excess momentum were given in [8]. Here we will consider only the case of negative excess momentum (when no jet was blown through the slit). The measurements were made at a free-stream velocity $U_\infty = 14$ m/sec, which corresponded to a Reynolds number $Re = U_\infty d / \nu = 9.3 \cdot 10^3$. Thanks to the deflection of the lower wall of the tunnel it was possible to ensure constancy of the velocity in the working section correct to $\pm 0.2\%$, except in the initial part of the section where the model was mounted. The degree of turbulence of the free stream at the inlet to the working section was equal to approximately 0.3%. The drag coefficient $C_x = 0.39$ was determined from the results of measurements of the average velocity profiles in the self-similar region of the wake with allowance for the degree of obstruction of the channel [7].

The average velocity was determined with a hot-wire anemometer and combined Pitot-Prandtl tube with an outside diameter of 2.7 mm and a total-head orifice diameter of 0.8 mm. The pressure drop at the tube was checked with an accuracy of 0.1 Pa using a MKV-250 micromanometer. The turbulence characteristics were measured with a DISA hot-wire anemometer apparatus incorporating 55D01 hot-wire anemometers, 55D10 linearizers, 55D26 filter units, a 55D35 effective value voltmeter, and a 55D70 correlator. The serially produced 55P01 and 55P61 probes had one or two crossed wires 5 μ m in diameter with a sensitive length of 1.2 mm. To measure the microscale we used an analog differentiator with a working frequency band extending from 0 to 40 kHz. The measured values of the microscale and the rate of dissipation of kinetic energy of turbulence were corrected for the effect of the limited resolution of the probes and of the background turbulence and apparatus noise, as in [9].

In order to estimate the universality of the functions f and g_{ij} in relations (1), the measured characteristics of the plane wake were made dimensionless by dividing by U_* and l_* (determined from (2)) and compared with the existing data for plane bodies of essentially different shape (circular [1, 10-12] and elliptic [6] cylinders and flat plates [13-15]).

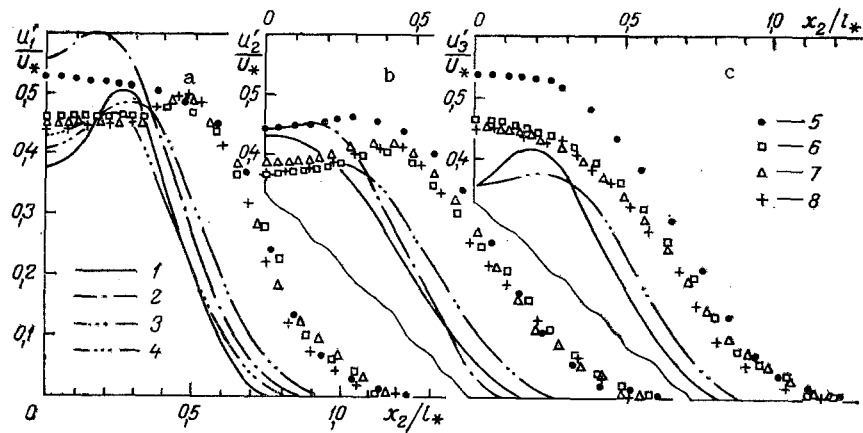


Fig. 2. Profiles of fluctuation velocity components u_1'/U_* (a), u_2'/U_* (b), u_3'/U_* (c): 1) circular cylinder [1]; 2) plate [3]; 3) circular cylinder [11]; 4) elliptic cylinder [6]; 5-8) authors' data ($x_1/d = 23, 32, 41,$ and $48,$ respectively).

Examination of the transverse distributions of the longitudinal component of the average velocity (Fig. 1a) shows that in the self-similar flow region the relative value of the velocity defect $\Delta U/U_*$ and the half-width of the wake may differ considerably depending on the body geometry. The wake formed behind the body investigated has the minimum velocity defect and the maximum width. It is characterized by the establishment of similarity of the $\Delta U/U_*$ profiles over relatively small distances ($x_1/d \geq 40$). In the case of a circular cylinder this distance is much greater ($x_1/d \geq 200$) [11]. It is interesting to note that differences in the $\Delta U/U_*$ profiles are observed even for circular cylinders, i.e., bodies of the same shape [1, 11]. Since the measurements were made at large distances from the cylinder ($x_1/d = 500$ and 400 , respectively), the noncoincidence of the profiles cannot be attributed to the incomplete self-similarity of the flow. The cause of the discrepancy is associated with differences in the experimental conditions with respect to such parameters as the free-stream turbulence, the surface roughness of the cylinder, its degree of elongation, the tunnel obstruction factor, etc.

In the flow in question, the self-similarity profile of the velocity defect differs in shape from the so-called universal profile observed in many types of jet flows and described by an exponential function. This is clear from comparing the profiles made dimensionless by dividing by the defect on the axis of symmetry $\Delta U/\Delta U_0$ [7]. For an elongated body with two sharp edges it is fuller at the apex and narrower in the outer region of the wake. The velocity profiles in the wakes of bluff bodies of revolution have a similar shape [3]. It may be assumed that this is associated with the presence of a separation zone behind a body with a flat base.

Figure 1b shows the nonuniversality of the dependence of $\Delta U_0/U_\infty$ on the longitudinal coordinate x_1/θ for various types of plane wakes. As the characteristic linear dimension of the flow we have chosen the momentum thickness:

$$\theta = \int_{-\infty}^{\infty} \frac{U}{U_\infty} \left(1 - \frac{U}{U_\infty}\right) dx_2. \quad (3)$$

For a cylinder in an unconfined flow θ is related to the drag coefficient by the simple expression: $C_x = 2\theta/d$. This quantity is convenient because at a certain distance from the body (when the pressure in the wake can be considered constant) it does not depend on distance. In the flow investigated the asymptotic law of decay of the velocity defect along the axis

$$\Delta U/U_\infty = C(x_1/\theta)^{-0.5} \quad (4)$$

will be valid at much smaller distances than in other plane wakes ($x_1/\theta = 80$, $x_1/d = 18$). The nonmonotonic variation of $\Delta U/U_\infty$ downstream at small distances from the body ($x_1/\theta \leq 12$), like the flattening of the velocity profile near the axis of symmetry, is attributable to the effect of the recirculation zone. The constant C in Eq. (4) is nonuniversal, as may be seen by comparing the data for various plane wakes in Fig. 1b.

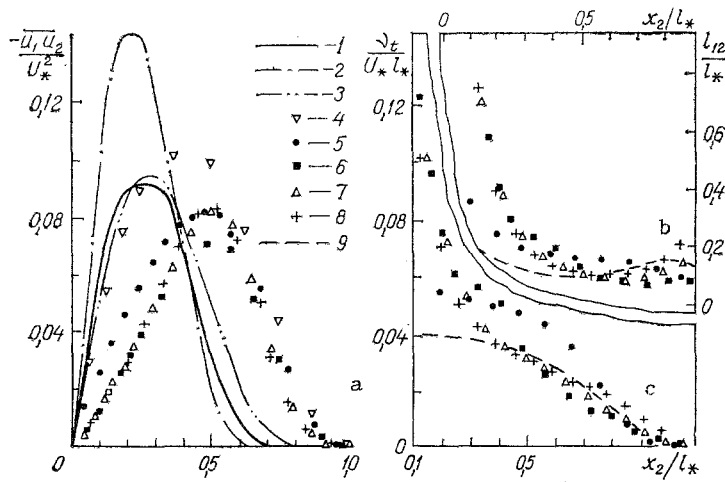


Fig. 3. Profiles of the turbulent shear stresses $-\overline{u_1 u_2}/U_*^2$ (a), mixing length l_{12}/l_* (b) and eddy viscosity $\nu_t^*/U_* l_*$ (c): 1) circular cylinder [10]; 2) plate [13]; 3) circular cylinder [11]; 4-8) authors' data ($x_1/d = 14, 23, 32, 41,$ and $48,$ respectively); 9) circular cylinder [16].

The effect of the body shape on the characteristics of the self-similar wake is also manifested in the profiles of the fluctuation velocity components and the turbulent friction in Figs. 2 and 3a. Self-similarity of the investigated flow with respect to the fluctuation characteristics is observed at distances of about 40 calibers. For comparison we note that in the wake of a circular cylinder the region of self-similar development begins from distances $x_1/d > 500$ [1] and in the wake of an elliptic cylinder [6] from $x_1/d > 9$. From a comparison of the data for the various plane wakes it is clear that behind the elongated plane body with two sharp trailing edges the wake is not only markedly broader with respect to all the characteristics but is also distinguished by the shape of the fluctuation velocity component distributions. In this connection, the results of the measurements of the fluctuation characteristics in the wake of a circular cylinder reported in [1] and [11] do not coincide. The possible causes of the discrepancy, unrelated to the shape of the body, have already been mentioned in connection with the average velocity profiles.

On the basis of the measured values of the Reynolds shear stresses and the average velocity we calculated the values of the mixing length l_{12} :

$$l_{12} = (-\overline{u_1 u_2})^{0.5} / \frac{\partial U}{\partial x_2} \quad (5)$$

and the turbulent viscosity ν_t :

$$\nu_t = (-\overline{u_1 u_2}) / \frac{\partial U}{\partial x_2}, \quad (6)$$

which are used in simple semiempirical models of turbulence. In order to find the derivatives $\partial U/\partial x_2$ we approximated the measured velocity profiles by means of the expression

$$\Delta U = \Delta U_0 \exp(-0.1\eta^2 - 0.6\eta^4), \quad (7)$$

where $\eta = x_2/\delta_{0.5}$; $\delta_{0.5}$ is the half-width of the wake relative to the velocity profile. The transverse distributions of l_{12} and ν_t are given in Figs. 3b and c. Neither of these parameters can be considered constant or weakly varying, as is usually assumed in simple semiempirical models of turbulence. At the same time, for the self-similar wake of a circular cylinder, as may be seen from a comparison with the corresponding data of [16], such an assumption is better justified (at any rate near the axis for ν_t and in the region $0.3 < x_2/l_* < 0.9$ for l_{12}).

The profiles of the Taylor microscale λ , given by

$$\lambda = \left[\overline{u_1^2} / \left(\frac{\partial \overline{u_1}}{\partial x_1} \right)^2 \right]^{0.5}, \quad (8)$$

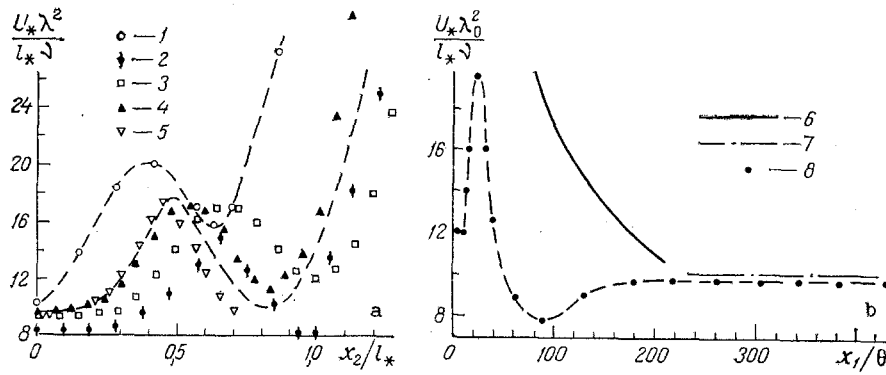


Fig. 4. Profiles (a) and variation along the wake axis (b) of the microscale: 1) circular cylinder [10]; 2-5) authors' data ($x_1/d = 23, 41, 59,$ and $84.5,$ respectively); 6) circular cylinder [14]; 7) circular cylinder [17]; 8) authors' data.

are reproduced in Fig. 4a. They are similar at $x_1/d \geq 40$ and differ somewhat in shape from the self-similar λ profile in the wake of a circular cylinder [10]. As far as the variation of λ_0 downstream is concerned, as is known, in the self-similar flow region (where equilibrium is established between the various components of the kinetic turbulent energy balance) we have

$$\lambda_0^2 = C_1 (x_1/\theta). \quad (9)$$

From relations (9), (1), and (2) it follows that in the self-similar plane wake the dimensionless parameter $\lambda_0^2 U_* / l_* \nu$ does not depend on x_1 . The data presented in Fig. 4b show that in the near zone of the flow investigated this parameter varies nonmonotonically and over a wide range; however, starting from distances $x_1/d = 180$, it takes a constant value of 9.8. A similar value ($\lambda_0^2 U_* / l_* \nu = 10$) was obtained in the wake of a circular cylinder [17], and in the self-similar region it is independent not only of x_1 but also of the Reynolds number. The available information on the microscale is too limited for it to be possible to estimate the extent to which in the self-similar plane wake the parameter $\lambda_0^2 U_* / l_* \nu$ depends on the shape of the body. In particular, the data of [14] reproduced in Fig. 4b relate to the non-self-similar region of the wake behind a circular cylinder and therefore do not permit the determination of the asymptotic value of the parameter in question.

In the experimental determination of the rate of dissipation of turbulent energy ϵ it is usual to employ a locally isotropic approximation relating ϵ with the measured values of u_1^2 and λ :

$$\epsilon = 15\nu \overline{(\partial u_1 / \partial x_1)^2} = 15\nu u_1^2 / \lambda^2. \quad (10)$$

In order to estimate the accuracy of the approximation (10) in the self-similar region of the flow investigated we made use of the known integral relation [1]:

$$U_\infty \frac{d}{dx_1} \int_0^\infty (\Delta U^2 + q^2) dx_2 = -2 \int_0^\infty \epsilon dx_2, \quad (11)$$

which, taking into account the self-similarity of the ΔU , q^2 , and ϵ profiles, can be brought into the form:

$$\int_0^\infty (\Delta U^2 + q^2) dx_2 = \frac{4l_*}{U_*} \int_0^\infty \epsilon dx_2. \quad (12)$$

Calculations using the experimental data showed that the left side of expression (12) is approximately 8% greater than the right, which testifies to the reliability of the measurements of the average and fluctuation values and the admissibility of using the locally isotropic relation (10) for estimating the rate of dissipation of turbulent energy in the self-similar region of the plane wake.

NOTATION

U , longitudinal average velocity; u_i , fluctuation velocity component; $\overline{u_i u_j}$, Reynolds stresses; $q^2 = u_i u_i$, twice the kinetic energy of turbulence; $\epsilon = \nu \overline{(\partial u_1 / \partial x_k)^2}$, rate of dissipation of turbulent energy; d is the maximum vertical dimension of the body; x_1 , streamwise

coordinate; x_2 , vertical coordinate; λ , Taylor microscale; ν , kinematic viscosity coefficient; U_* and ℓ_* , characteristic velocity and length scales defined by (2). Subscripts: 0 denotes the centerline value, ∞ the free-stream value, and ()' the root-mean-square value.

LITERATURE CITED

1. A. A. Townsend, Structure of Turbulent Shear Flow [Russian translation], Moscow (1959).
2. H. Schlichting, Boundary Layer Theory [Russian translation], Moscow (1974).
3. H. Reichardt and R. Ermshaus, Int. J. Heat Mass Transfer, 5, 251-265 (1962).
4. V. I. Bukreev, O. V. Vasil'ev, and Yu. M. Lytkin, Dokl. Akad. Nauk SSSR, 207, No. 4, 804-807 (1972).
5. P. M. Bevilagua and P. S. Lykoudis, J. Fluid Mech., 89, Pt. 3, 589-606 (1978).
6. Yu. M. Lytkin, in: Continuum Dynamics [in Russian], Novosibirsk (1970), No. 5, pp. 51-55.
7. P. Ya. Cherepanov, in: Turbulent Transport Processes [in Russian], Minsk (1985), pp. 56-74 (Coll. Sci. Proc. Inst. Heat and Mass Transfer AS BSSR).
8. Yu. M. Dmitrenko, I. I. Kovalev, N. N. Luchko, and P. Ya. Cherepanov, Inzh.-Fiz. Zh., 52, No. 5, 743-751 (1987).
9. B. A. Kolovandin, N. N. Luchko, Yu. M. Dmitrenko, and V. L. Zhdanov, Minsk (1982), (Preprint No. 10, Inst. Heat and Mass Transfer AS BSSR).
10. A. A. Townsend, Proc. R. Soc. Ser. A, 197, No. 1049, 124-132 (1948).
11. G. Fabris, J. Fluid Mech., 94, Pt. 4, 673-709 (1979).
12. L. N. Ukhanova, in: Industrial Aerodynamics, No. 27 [in Russian] (1966), pp. 83-95.
13. R. Chevray and L. S. G. Kovaszny, AIAA J., No. 8, 1641-1643 (1969).
14. A. N. Sekundov and O. V. Yakovlevskii, Izv. Akad. Nauk SSSR, Mekh. Zhidk. Gaza, No. 6, 131-137 (1970).
15. P. J. Pot, Data Report, NLRTR-79063U, Netherlands (1979).
16. H. Yamada, Y. Kuwata, H. Osaka, and Y. Kageyama, Technology Reports, Yamaguchi Univ. (1980), Vol. 2, No. 4, pp. 329-339.
17. M. S. Uberoi and P. Freymuth, Phys. Fluids, 12, No. 7, 1359-1363 (1969).

INVESTIGATION OF LOCAL HEAT TRANSFER ASSOCIATED WITH THE EVAPORATION OF A LIQUID FILM ON A HORIZONTAL RIBBED TUBE

Yu. V. Putilin, V. G. Rifert,
V. L. Podbereznyi, and P. A. Barabash

UDC 536.423.1

The heat-transfer enhancement effect of longitudinal ribs on a horizontal tube is discussed on the basis of experimental data on the local heat-transfer coefficients.

In [1] measurements of the mean heat-transfer coefficients for film flow over horizontal, longitudinally profiled tubes demonstrated the possibility of a 1.5-2-fold intensification of the heat transfer as compared with a smooth tube.

In order to investigate the mechanism of the heat-transfer process associated with film flow over a profiled tube, we made an experimental determination of the local heat-transfer coefficients. The experiments were carried out on an apparatus previously used to investigate the heat transfer associated with the evaporation of a film preheated to the saturation point on a smooth tube [2].

The experimental tubes had an outside diameter of 38 mm. As in [2], for measuring the mean wall temperature we used resistance microthermometers, arranged as shown in Fig. 1.

The microthermometers are conventionally represented by dots numbered 1-10. Into each profiled test piece we fitted 10 microthermometers in two groups of five, each of which

Kiev Polytechnic Institute. Translated from Inzhenerno-Fizicheskii Zhurnal, Vol. 54, No. 6, pp. 919-924, June, 1988. Original article submitted January 4, 1987.